



A potential game approach to multiple UAV cooperative search and surveillance

Pei Li^{a,b}, Haibin Duan^{a,b}

^a State Key Laboratory of Virtual Reality Technology and Systems, Beihang University, Beijing 100191, China

^b Bio-inspired Autonomous Flight Systems (BAFS) Research Group, School of Automation Science and Electrical Engineering, Beihang University, Beijing 100191, China

ARTICLE INFO

Article history:

Received 28 April 2016

Received in revised form 29 March 2017

Accepted 22 May 2017

Available online xxxx

Keywords:

Cooperative search

Potential game

Binary log-linear learning

Multiple unmanned aerial vehicles

Optimal coverage

ABSTRACT

In this paper, we developed a game theoretic formulation for multiple unmanned aerial vehicle (UAV) cooperative search and surveillance. The cooperative search problem is decomposed into three sequential tasks: coordinated motion, sensor observation, and cooperative information fusion. Firstly, the coordinated motion is designed as a multi-player potential game with constrained action sets. Then the binary log-linear learning is adopted to perform motion control, which guarantees optimal coverage. Then a consensus based fusion algorithm is introduced to construct the probability map to guide the following coordinated motion. Finally, simulations are performed to validate the effectiveness of our proposed approach. The modular framework enables the separate design of utility functions and learning algorithms, which offers a flexible way to accommodate different global objectives and underlying physical constraints.

© 2017 Elsevier Masson SAS. All rights reserved.

1. Introduction

Many search and surveillance missions involve measuring and exploring an unknown region, such as target detection [1,2], environmental monitoring [3,4], and map building [5,6]. In recent years, the unmanned aerial vehicles (UAVs) have drawn much attention in cooperative search problems owing to their increasing autonomy. Apparently, greater efficiency can be achieved in information collection with teams of autonomous UAVs operating in a coordinated fashion [7–13]. The cooperative search involves the design of distributed algorithms that use the localized information to achieve a globally optimized objective for systems composed of interconnected components. Several challenges are deserving to be addressed in cooperative search problems using multiple vehicles [14–16]. Firstly, individuals are required to operate (move and sense) autonomously with limited sensing and communication capabilities [17–20]. Secondly, the system should be designed to provide the network with adaptation and robustness to unexpected situations. Thirdly, consideration must be given to issues of different global objectives and underlying constraints.

A provably convergent Kalman filter combining sensor observations is developed in [21] to explore the scalar field. The optimal formation shape can be achieved by applying estimations from

the designed filter into the motion control law. Along with the consensus-based fusion algorithm, a path planning algorithm is proposed based on centroidal Voronoi partitioning to realize a final optimal configuration in [22]. In [23], a self-assessment based decision-making method is designed for cooperative search under various communication structures. This approach shows some attractive features such as less computational complexity, low communication overheads, and excellent scalability. The designed control system in [12] consists of three parallel components: coverage control, data source detection, and data collection. Operations in environments with obstacles are especially important for urban monitoring or disaster management. However, additional efforts are often required to deal with the discontinuities imposed by the obstacles. Moreover, most studies focus on cooperative search with the assumption that UAVs involved in the mission are homogeneous.

The relevance of game theory to cooperative control has been recognized due to the fact that game theory concerns the study of interacting decision makers. Especially, the potential game is beginning to emerge as a valuable paradigm for cooperative control [24,25]. The important aspect of potential games lies in that the potential function guarantees utilities of the individuals are localized to themselves yet aligned with the global objective. Motivated by these facts, we developed a potential game approach to accommodate the challenges imposed by cooperative search problems. In our study, the cooperative search problem is decomposed into

E-mail address: hbduan@buaa.edu.cn (H. Duan).

<http://dx.doi.org/10.1016/j.ast.2017.05.031>

1270-9638/© 2017 Elsevier Masson SAS. All rights reserved.

Nomenclature

1	UAVs	Unmanned aerial vehicles	67
2	Ω	Mission area	68
3	n	Number of UAVs	69
4	V, S	Set of vehicles and set of players	70
5	v_i	The i th UAV, $i = 1, 2, \dots, n$	71
6	t	Time step	72
7	g	Position of the partitioned cell	73
8	C_i, μ_i	Sensing area and position of vehicle v_i	74
9	R_{S_i}, R_{C_i}	The sensing range and the communication range of vehicle v_i	75
10	Net	Graph of the UAV network	76
11	E	The edge set of graph Net	77
12	N_i, κ_i	The neighbor set and the degree of vehicle v_i	78
13	G	Strategic form game	79
14	A_i, U_i	The action set and utility function of player i	80
15	a, \tilde{a}, a'	Joint actions of the players	81
16	a_i, \tilde{a}_i, a'_i	Action of player i	82
17	a_{-i}	Action profile of players other than player i	83
18	a^*	Joint actions of the players at the Nash Equilibrium	84
19	Φ	The potential function of game G	85
20	η	The density function	86
21	f	The function of signal degradation	87
22			88
23			89
24			90
25			91
26			92
27			93
28			94
29			95
30			96
31			97
32			98
33			99
34			100
35			101
36			102
37			103
38			104
39			105
40			106
41			107
42			108
43			109
44			110
45			111
46			112
47			113
48			114
49			115
50			116
51			117
52			118
53			119
54			120
55			121
56			122
57			123
58			124
59			125
60			126
61			127
62			128
63			129
64			130
65			131
66			132

three tasks: coordinated motion, sensor observation, and information fusion. On the one hand, UAVs autonomously perform coordinated movements to reach an optimal configuration that maximizes the event detection probability. On the other hand, UAVs gather information from observations to construct a probability map and fuse information through interactions with its neighboring UAVs.

The main contribution of this paper is the development of a potential game formulation for cooperative search. By designing the cooperative search as a potential game, UAVs equipping with isotropic sensors are viewed as autonomous decision makers. The binary log-linear learning is adopted to perform motion control with a simplified kinetic model, which guarantees optimal coverage [26]. Sufficient conditions regarding sensing and communication capabilities are given for implementing this learning algorithm. The modular framework enables the separate design of utility functions and learning algorithms, which offers a flexible way to accommodate different global objectives and underlying physical constraints. This potential game formulation makes it possible for UAVs to operate with heterogeneous sensors or even in the mission area with non-convex obstacles without introducing additional treatment. This capability is encoded into the constrained action sets implicitly. Besides, associated learning processes provide UAVs with robustness to failures caused by hardware malfunctions, software faults, or deliberate attacks. This approach can be used in applications of exploring an entirely unknown structured area, such as disaster management, and target detection in urban environments.

The remainder of this paper is structured as follows. Problem setup and some basic assumptions are provided in Section 2. By formulating cooperative search as a potential game, we adopt the binary log-linear learning for coordinated motion in Section 3. Moreover, sufficient communication conditions necessary for implementing this learning algorithm are also provided. Then the entire procedure of coordinated motion and cooperative information fusion to construct the probability map is described in Section 4. The effectiveness of our proposed approach is verified by comparative results in Section 5. The last section offers some concluding remarks.

$C_{a_i(t-1)}$	Constrained action set of player i at time t
z_i	Maximum number of actions in $C_{a_i(t-1)}$
$P(D)$	The probability of event D
$P(D E)$	The conditional probability of D given E
τ	Amplitude of noise in binary log-linear learning
$\pi(a)$	Probability distribution over state space of action a
$P_{a \rightarrow a'}$	State transition probability from action profile a to a'
\mathbf{P}	State transition matrix
d	Euclidean distance
θ_g	Event that a target is present in cell g
p_c, p_f	Detection probability and false alarm probability
$Z_{i,g,t}, P_{i,g,t}$	Measurement and target existence probability of vehicle v_i at time t for cell g
$H_{i,g,t}$	Nonlinear transformation of $P_{i,g,t}$
$Q_{i,g,t}$	Linear combination of $H_{i,g,t}$
W	Metropolis weight matrix
$\omega_{i,j,t}$	Weight on $H_{j,g,t}$ for vehicle v_i
k_η	Positive gain
$\bar{\eta}$	Average uncertainty of all the vehicles
δ_0	Predefined threshold for termination
F_S	Sampling frequency

2. Problem setup and some basic definitions

In this section, procedures for performing a search operation are described briefly to provide an overall view of this problem. Then we introduce some basic definitions and assumptions about exploring an unknown area with multiple UAVs. Besides, some preliminary definitions of potential games are provided.

2.1. Problem formulation of cooperative search

Usually, the cooperative search problem involves the following three parts: coordinated motion, sensor observation, and information fusion. Before starting the search, each vehicle associates its knowledge of the mission space with a probability map. Then UAVs tend to move towards locations with high uncertainty to increase data gathering. After UAVs deploy themselves to new locations, they perform observations to detect data source and collect data. To further enhance the search effectiveness, UAVs usually carry out information fusion through communication with their neighbors, integrating both spatial and temporal estimation. Moreover, observations reduce the uncertainty over corresponding areas, which in turn guide the following coordinated motion. Then the entire procedure continues until the probability distribution over the whole mission space is bellowed a predetermined threshold, as is shown in Fig. 1.

2.2. Basic definitions and assumptions

Consider the problem of searching an unknown area $\Omega \in \mathbb{R}^2$ using n UAVs, labeled as $V = \{v_1, v_2, \dots, v_n\}$. Each vehicle acts as a self-interested decision maker to gain knowledge about the mission space (as shown in Fig. 2). The continuous area $\Omega \in \mathbb{R}^2$ is uniformly partitioned into equal cells and each cell is identified by the position of its center g . Each vehicle v_i independently takes measurements $Z_{i,g,t}$ over cells within its sensing range $C_i = \{g \mid |g - \mu_i| \leq R_{S_i}\}$, where R_{S_i} represents the sensing range of v_i . Also note that, for simplicity sake, we suppose the signal over cell g could be wholly observed by v_i when its center is within C_i . Only two results can be observed when v_i carries out a measurement, that is, $Z_{i,g,t} = 1$ if $|g - \mu_i| \leq R_{S_i}$, or $Z_{i,g,t} = 0$ if $|g - \mu_i| > R_{S_i}$.

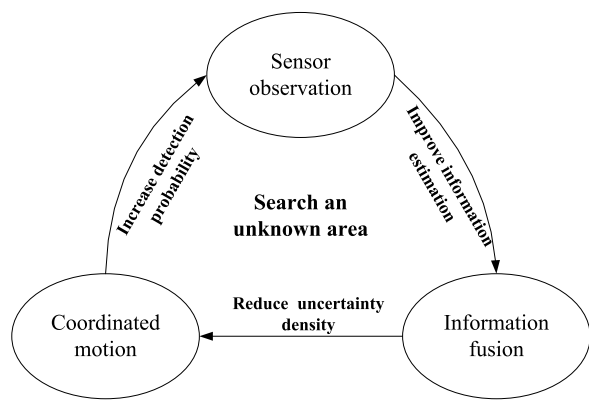


Fig. 1. Procedures of cooperative search using multiple UAVs.

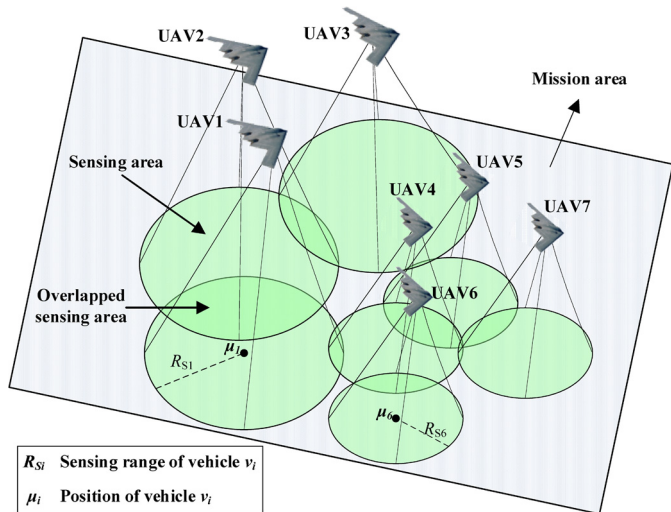


Fig. 2. Schematic of cooperative search using multiple UAVs.

Here we model the mobile UAVs as a dynamic graph $Net = (E, V)$ consisting of a vertex (vehicle) set $V = \{v_1, v_2, \dots, v_n\}$ and an edge set $E = \{(v_i, v_j) : v_i, v_j \in V; \|\mu_i - \mu_j\| \leq R_{C_i}\}$, where μ_i and μ_j are positions of two distinct UAVs v_i and v_j , and R_{C_i} is the communication range of v_i . Here by denoting the neighbor set of v_i as $N_i = \{v_j \in V | (v_i, v_j) \in E\} \cup \{v_i\}$, we take the standard assumption that a vehicle is a neighbor of itself. The degree of v_i is denoted as $\kappa_i = |N_i|$.

2.3. Preliminaries: potential games

The potential game is a kind of game that plays a prominent role in the cooperative control of distributed multi-agent systems [24,27,28], stemming from the fact that it guarantees each player's localized utility is aligned with the global objective. Here we first introduce some basic definitions about potential games.

A strategic form game $G(S, \{A_i, i \in S\}, \{U_i, i \in S\})$ is characterized by the following three components: (1) a set of players $S = \{1, 2, \dots, n\}$, (2) a set of joint actions $\{A_i, i \in S\}$, where A_i is the set of actions available to player i , and (3) a set of utility functions $\{U_i, i \in S\}$, where $U_i : A_i \rightarrow \mathbf{R}$ is the utility function for player i . In the strategic game, $a = (a_1, a_2, \dots, a_n)$ represents the joint actions of the players. We use the notation $a = (a_i, a_{-i})$, where a_{-i} denotes the action profile of the players other than player i . Accordingly, we may refer to $U_i(a)$ as $U_i(a_i, a_{-i})$.

Definition 1 (Exact Potential Games [28]). A game $G(S, \{A_i, i \in S\}, \{U_i, i \in S\})$ is called an exact potential game if there exists a global function $\Phi : A \rightarrow \mathbf{R}$ such that,

$$U_i(a'_i, a_{-i}) - U_i(a_i, a_{-i}) = \Phi(a'_i, a_{-i}) - \Phi(a_i, a_{-i}), \quad \forall i \in S, a_i, a'_i \in A_i, a_{-i} \in A_{-i}, \quad (1)$$

where the global function Φ is known as the potential function of game G . Following the common practice, we will henceforth refer to exact potential games simply as potential games.

Definition 2 (Nash Equilibrium [29]). A strategy $a^* = (a_i^*, a_{-i}^*)$ is called a Nash Equilibrium of game $G(S, \{A_i, i \in S\}, \{U_i, i \in S\})$, if and only if

$$U_i(a_i^*, a_{-i}^*) \leq U_i(a_i, a_{-i}^*), \quad \forall i \in S, \forall a_i \in A_i. \quad (2)$$

As we can see from the definition of potential games, a unilateral better reply for player i increases the potential function Φ . It cannot perpetually increase if the players have finite states and any action profile maximizing Φ leads to a pure Nash equilibrium. Hence, at least one such equilibrium exists in the potential game. Consequently, a potential game may possess several Nash Equilibria [30], i.e., there may exist some suboptimal pure Nash equilibria that do not maximize the potential function.

3. A potential game approach to coordinated motion

In this section, we formulate this problem as a potential game by designing proper individual utilities for UAVs. Then we adopt the binary log-linear learning as the underlying learning algorithm, which is suitable for real-time implementation and guarantees asymptotic convergence to the optimal configuration. We have also provided sufficient communication conditions for UAVs to evaluate expected utilities, which is necessary for this game theoretic learning. This potential game formulation makes it possible for UAVs to operate with heterogeneous sensors or even in the mission area with obstacles.

3.1. Coordinated motion formulated as a potential game with constrained action sets

We start the design by viewing n UAVs as players negotiating to reach a desirable state of the whole group. First, we model this problem as a multiplayer game with constrained action sets. Then we design appropriate vehicle utilities to capture both alignment and localization by taking advantage of marginal contribution utility, or often referred to as wonderful life utility [31], which constitutes a potential game.

Next, we will design the action set A_i of each player $v_i \in V$. We have noticed that the performance of UAVs depends on their positions. Hence, A_i could be defined as a finite set of locations that a player could select, that is, $A_i = \{g | g \in \Omega\}, \forall v_i \in V$. Here the kinetic dynamics of UAVs are simplified as constrained action sets since we mainly focus on the coordination strategy. The action of v_i is denoted by $a_i \in A_i$, and the collective actions of the vehicle network are defined as $a = (a_1, a_2, \dots, a_n)$, called the action profile. The set of actions available to v_i at time t is a function of his action at time $t-1$, denoted as constrained set $C_{a_i(t-1)} \subseteq A_i$ (as is shown in Fig. 3). Note that $a_i(t-1) \in C_{a_i(t-1)}$ since we assume that a vehicle is allowed to stay with its previous location.

In this process, a density map $\eta(g) : \Omega \rightarrow \mathbf{R}_+$ could be utilized to represent the event occurrence probability. Due to the loss of signal strength [14], the sensing performance usually decays with $\|g - \mu_i\|$. Here we describe this degradation using a non-decreasing differentiable function $f(\|g - \mu_i\|) : \mathbf{R}_+ \rightarrow \mathbf{R}_+$. The

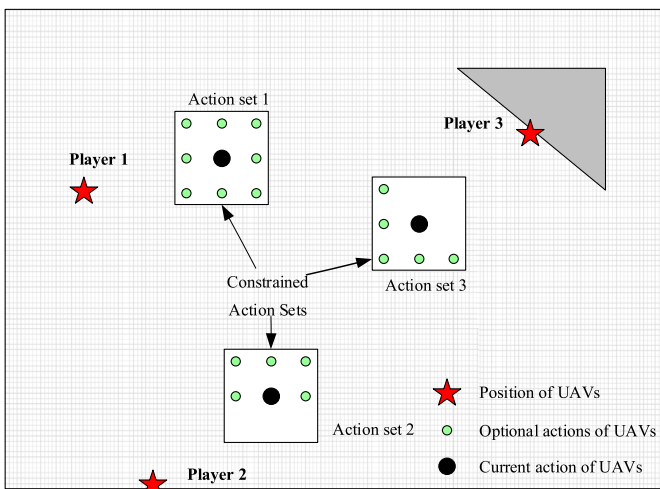


Fig. 3. Constrained action sets of vehicles.

overall performance of UAVs can be measured by the function of density and signal degradation as follows

$$\Phi(a) = \Phi(\mu_1, \mu_2, \dots, \mu_n) = \int_{\Omega} f\left(\min_{i \in \{1, 2, \dots, n\}} \|g - \mu_i\|\right) \eta(g) dg \quad (3)$$

where

$$f(\|g - \mu_i\|) = \begin{cases} \|g - \mu_i\| & \|g - \mu_i\| \leq R_S \\ 0 & \text{otherwise} \end{cases}$$

and $\eta(g)$ is the density function.

In the context of this paper, the utility of v_i is designed as its marginal contribution to the global utility [24,31], which takes the form

$$U_i(a_i, a_{-i}) = \int_{\Omega} f\left(\min_{i \in \{1, 2, \dots, n\}} \|g - \mu_i\|\right) \eta(g) dg - \int_{\Omega} f\left(\min_{i \in \{1, 2, \dots, i-1, i+1, \dots, n\}} \|g - \mu_i\|\right) \eta(g) dg. \quad (4)$$

Lemma 1. Consider a coverage problem formulated as a multiplayer game, where $V = \{v_1, v_2, \dots, v_n\}$ is the set of players, and $A = A_1 \times A_2 \times \dots \times A_n$ is the set of joint actions. If player v_i takes $U_i(a_i, a_{-i})$ defined by Eq. (4) as its individual utility, then it constitutes a potential game with the potential function $\Phi(a)$ defined by Eq. (3).

Proof. Let $a_i = \mu_i$ and $a'_i = \mu'_i$ be two possible actions for v_i , and let a_{-i} denote actions of the remaining players. Note that Eq. (4) can be rewritten as

$$U_i(a_i, a_{-i}) = \Phi(a_i, a_{-i}) - \int_{\Omega} f\left(\min_{i \in \{1, 2, \dots, i-1, i+1, \dots, n\}} \|g - \mu_i\|\right) \eta(g) dg. \quad (5)$$

Using Eq. (5), we get,

$$\begin{aligned} U_i(a'_i, a_{-i}) - U_i(a_i, a_{-i}) &= \Phi(a'_i, a_{-i}) - \Phi(a_i, a_{-i}) - (\Phi(a_i, a_{-i}) - \Phi(a_{-i})) \\ &= \Phi(a'_i, a_{-i}) - \Phi(a_i, a_{-i}). \end{aligned} \quad (6)$$

From the definition of potential games, the formulated multiplayer game for coverage control taking Eq. (4) as individual utility

leads to a potential game with the potential function defined by Eq. (3). \square

In this condition, each vehicle seeks to optimize its own objective selfishly, leading to an improvement in the overall performance benefiting from the unique properties of potential games. Moreover, it is convenient for a vehicle to calculate the expected utility when it takes an admissible action through local interaction. Especially, this desirable feature makes the individual utility more learnable under some communication conditions, which will be addressed in detail in the following.

Remark 1. As we can see from Eq. (3), the search effectiveness function consists of two terms, denoted as $f(\|g - \mu_i\|)$ and $\eta(g)$, respectively. One should notice that $f(\cdot)$ can be adjusted appropriately to describe the inherent properties of different sensors. For example, it is defined as $\|\mu_i - g\|^2$ in [14]. UAVs seek to maximize the coverage when performing a surveillance mission and η represents the target existence probability. UAVs seek to maximize the reduction in uncertainty when performing a search mission and η can be designed as an uncertainty function. Importantly, η can either be given as a predefined function or updated dynamically in various ways. In our study, it is updated dynamically using the fused information, which will be discussed in detail in Section 5.

3.2. Binary log-linear learning for optimal coverage

Various learning algorithms have been proposed to explore the equilibrium in games, such as fictitious play [32], best-response learning [33]. Especially, log-linear learning, originally proposed by Blume [31,34], guarantees convergence to the optimal Nash equilibrium. The drawback of log-linear learning lies in that UAVs need to compute utilities of all possible actions. So here we adopt the binary log-linear learning as the underlying algorithm, which can be applied with less computational burdens and is suitable for real-time operations [26].

In binary log-linear learning, a vehicle $v_i \in V$ is randomly selected to change its location with equal probability. In practical implementations, the selection of v_i can be achieved by adopting the asynchronous time model in [35]. We assume that the remaining UAVs repeat their previous actions, i.e., $a_{-i}(t) = a_{-i}(t-1)$. Then v_i is allowed to choose one trial action a'_i from its constrained action set $C_{a_i(t-1)}$ to alter its position with the following probability [24],

$$\begin{cases} P(a'_i = a_i) = 1/z_i, & \text{for } a_i \in C_{a_i(t-1)} \setminus a_i(t-1) \\ P(a'_i = a_i(t-1)) = 1 - (|C_{a_i(t-1)}| - 1)/z_i &end{cases} \quad (7)$$

where z_i denotes the maximum number of actions in $C_{a_i(t-1)}$, i.e., $z_i = \max_{a_i \in A_i} |C_{a_i(t-1)}|$.

After vehicle v_i selects a trial action, it updates its action at time t according to the following strategy [26],

$$\begin{cases} P(a_i(t) = a_i(t-1)) = \frac{e^{\frac{1}{\tau} U_i(a(t-1))}}{e^{\frac{1}{\tau} U_i(a(t-1))} + e^{\frac{1}{\tau} U_i(a'_i, a_{-i}(t-1))}} \\ P(a_i(t) = a'_i) = \frac{e^{\frac{1}{\tau} U_i(a'_i, a_{-i}(t-1))}}{e^{\frac{1}{\tau} U_i(a(t-1))} + e^{\frac{1}{\tau} U_i(a'_i, a_{-i}(t-1))}} \end{cases} \quad (8)$$

where $P(a_i(t) = a_i(t-1))$ and $P(a_i(t) = a'_i)$ represent the probability that v_i would select action $a_i(t-1)$ and trial action a'_i . And $U_i(a(t-1))$ and $U_i(a'_i, a_{-i}(t-1))$ are its current utility and the expected utility it would receive by playing a'_i , respectively. The temperature τ determines the amplitude of noise, indicating how likely a vehicle is to take a suboptimal action. A vehicle would select the best response action with arbitrarily high probability as $\tau \rightarrow 0$.

Proposition 1 (Reachability). For any vehicle $v_i \in V$ and any action pair $a_i(0), a_i(m) \in A_i$, there exists a sequence of actions $a_i(0) \rightarrow a_i(1) \rightarrow \dots \rightarrow a_i(m)$ such that $a_i(t) \in C_{a_i(t-1)}$ for all $t \in \{1, 2, \dots, m\}$.

Proposition 2 (Reversibility). For any vehicle $v_i \in V$ and any action pair $a_i, a'_i \in A_i, a'_i \in C_{a_i} \Leftrightarrow a_i \in C_{a'_i}$.

Theorem 1. Consider the coordinated motion problem for optimal coverage formulated as a potential game with the potential function defined by Eq. (3), where all the players adhere to binary log-linear learning. If the designed constrained action sets meet the requirements of Proposition 1 and Proposition 2, the coverage performance $\Phi(a)$ will be maximized asymptotically with sufficient large time t , provided that $\tau \rightarrow 0$, i.e., $\lim_{t \rightarrow 0, t \rightarrow \infty} P(a = \arg \max_{\tilde{a} \in A} \Phi(\tilde{a})) = 1$.

Proof. As we can see from Lemma 1, the coordinated motion problem for optimal coverage defines a potential game. Here we will first prove that the binary log-linear learning induces a Markov process, which has a unique stationary distribution over state space, $\pi(a) \in \Delta(A)$, where

$$\pi(a) = \frac{e^{\frac{1}{\tau} \Phi(a)}}{\sum_{\tilde{a} \in A} e^{\frac{1}{\tau} \Phi(\tilde{a})}}, \quad \forall a \in A. \quad (9)$$

If the constrained action sets $C_{a_i(t-1)}$ satisfy Proposition 1 and Proposition 2, then the Markov process induced by binary log-linear learning is irreducible and aperiodic. Therefore, binary log-linear learning gives rise to a unique stationary distribution. Next, we will show that the unique distribution is precisely the one defined by Eq. (9).

Then, we will verify that the process determined by the distribution shown in Eq. (9) is reversible, i.e., for any $a, a' \in A$, we have $\pi(a)P_{a \rightarrow a'} = \pi(a')P_{a' \rightarrow a}$, where $P_{a \rightarrow a'} = P(a(t) = a'|a(t-1) = a)$. Especially, we focus the case where a' and a differ by exactly one player v_i , i.e. $a' = (a'_i, a_{-i})$ and $a = (a_i, a_{-i})$, where $a'_i \in C_{a_i}$, which also implies $a_i \in C_{a'_i}$. It is easy for us to check that

$$\begin{aligned} \pi(a)P_{a \rightarrow a'} &= \left\{ \frac{e^{\frac{1}{\tau} \Phi(a)}}{\sum_{\tilde{a} \in A} e^{\frac{1}{\tau} \Phi(\tilde{a})}} \right\} \left\{ \frac{(1/n)(1/z_i)e^{\frac{1}{\tau} U_i(a'_i, a_{-i})}}{e^{\frac{1}{\tau} U_i(a'_i, a_{-i})} + e^{\frac{1}{\tau} U_i(a_i, a_{-i})}} \right\} \\ &= ce^{\frac{1}{\tau} (\Phi(a) + U_i(a'_i, a_{-i}))} \end{aligned} \quad (10)$$

where

$$c = \frac{(1/n)(1/z_i)}{\left(\sum_{\tilde{a} \in A} e^{\frac{1}{\tau} U_i(\tilde{a})} \right) \left(e^{\frac{1}{\tau} U_i(a'_i, a_{-i})} + e^{\frac{1}{\tau} U_i(a_i, a_{-i})} \right)}.$$

Using the property of potential games, we have

$$U_i(a'_i, a_{-i}) - U_i(a) = \Phi(a'_i, a_{-i}) - \Phi(a). \quad (11)$$

By substituting the above function into Eq. (10), we can obtain

$$\begin{aligned} ce^{\frac{1}{\tau} (\Phi(a) + U_i(a'_i, a_{-i}))} &= ce^{\frac{1}{\tau} (\Phi(a'_i, a_{-i}) + U_i(a))} \\ &= \left(\frac{e^{\frac{1}{\tau} \Phi(a'_i, a_{-i})}}{\sum_{\tilde{a} \in A} e^{\frac{1}{\tau} \Phi(\tilde{a})}} \right) \left(\frac{(1/n)(1/z_i)e^{\frac{1}{\tau} U_i(a)}}{e^{\frac{1}{\tau} U_i(a'_i, a_{-i})} + e^{\frac{1}{\tau} U_i(a_i, a_{-i})}} \right) \\ &= \pi(a')P_{a' \rightarrow a}. \end{aligned} \quad (12)$$

In this way, we have $\pi(a)P_{a \rightarrow a'} = \pi(a')P_{a' \rightarrow a}$. Since we have proved that the Markov process is reversible with a distribution shown as Eq. (9), here we will prove that Eq. (9) is a stationary distribution by verifying that $\pi(a)$ is a fixed point. Let $\pi_t = \mathbf{P}\pi_{t-1}$, where π_{t-1} represents the probability distribution at time t and \mathbf{P} is the transition probability matrix at time $t-1$. Then

$$\pi_t(y) = \sum_{x \in A} \pi_{t-1}(x)P_{x \rightarrow y} = \sum_{x \in A} \pi_{t-1}(y)P_{y \rightarrow x} = \pi_{t-1}(y). \quad (13)$$

We could conclude that $\pi(a)$ is the unique stationary distribution. In this way, if all the players adhere to binary log-linear learning, it follows that

$$\lim_{\tau \rightarrow 0, t \rightarrow \infty} P\left\{ a = \arg \max_{\tilde{a} \in A} \Phi(\tilde{a}) \right\} = 1. \quad (14)$$

Hence, the coverage performance will be maximized asymptotically with sufficient large time t , provided that $\tau \rightarrow 0$. \square

3.3. Sufficient sensing and communication conditions for practical implementation

In the learning process, each vehicle should be able to evaluate the expected utility $U_i(a'_i, a_{-i})$ that it would have received if it selected an alternative action $a'_i \in A_i$. In this way, sufficient communication capabilities are required to ensure proper estimation of overlapped sensing areas. Here we will demonstrate sufficient communication conditions to implement the game theoretic learning.

Lemma 2. Let $V = \{v_1, v_2, \dots, v_n\}$ be a networked group of UAVs, and each vehicle $v_i \in V$ has a sensing range R_{S_i} and a communication range R_{C_i} . For any action profile $a \in A$, vehicle v_i located at μ_i can distinguish whether cell g can be observed by other UAVs if it satisfies that

$$d(\mu_i, g) \leq \min_{j=1,2,\dots,n} (R_{C_j} - R_{S_j}) \quad (15)$$

where $d(\mu_i, g)$ is the Euclidean distance between v_i and cell g .

Proof. Considering a vehicle v_k located at μ_k and a cell g within the sensing range of v_k , we have the following equation from triangle inequality,

$$d(\mu_i, \mu_k) \leq d(\mu_i, g) + d(\mu_k, g). \quad (16)$$

By noticing the fact that position of cell g falls within the sensing range of vehicle v_k , we obtain $d(\mu_k, g) \leq R_{S_k}$. Substituting the above equation and Eq. (15) into Eq. (16), we get

$$d(\mu_i, \mu_k) \leq \min_{j=1,2,\dots,n} (R_{C_j} - R_{S_j}) + R_{S_k}. \quad (17)$$

It is straightforward to check $\min_{j=1,2,\dots,n} (R_{C_j} - R_{S_j}) \leq R_{C_k} - R_{S_k}$. Then we have

$$d(\mu_i, \mu_k) \leq R_{C_k} - R_{S_k} + R_{S_k} = R_{C_k} \quad (18)$$

which implies that v_i is within the communication range of v_k .

To this end, if Eq. (15) is satisfied, then v_i is within the communication range of any vehicle covering g , that is, $d(\mu_i, \mu_k) \leq R_{C_k}, \forall v_k \in V$. Consequently, vehicle v_i located at μ_i can distinguish whether cell g can be observed by other UAVs. \square

Lemma 3. Let $V = \{v_1, v_2, \dots, v_n\}$ be a networked group of UAVs, and each vehicle $v_i \in V$ has a sensing range R_{S_i} and a communication range R_{C_i} . Vehicle v_i can calculate $U_i(a'_i, a_{-i}(t))$ for any action $a'_i \in C_{a_i(t-1)}$ if

$$R_{C_j} - R_{S_j} \geq \max_{j=1,2,\dots,n} R_{S_j} + 1, \quad \forall v_i \in V. \quad (19)$$

Proof. Considering the constraints of UAVs' mobile capability, we could find that an updating vehicle v_i can be at most be one hop away from its current position in the next time step. In other words, cells in its coverage set in the next time step

are at most $R_{S_i} + 1$ away from its current position μ_i . Hence, the cell g covered by vehicle v_i satisfies $d(\mu_i, g) \leq R_{S_i} + 1 \leq \max_{j=1,2,\dots,n} R_{S_j} + 1$ since for any vehicle v_i we have $R_{S_i} \leq \max(R_{S_j})$. Then if $\min_{j=1,2,\dots,n} (R_{C_j} - R_{S_j}) \geq \max_{j=1,2,\dots,n} R_{S_j} + 1$ holds, we have

$$d(\mu_i, g) \leq \min_{j=1,2,\dots,n} (R_{C_j} - R_{S_j}). \quad (20)$$

From Lemma 2, we know that vehicle v_i located at μ_i knows whether cell g is covered by other UAVs. In other words, v_i can compute $U_i(a'_i, a_{-i}(t))$ for any action $a'_i \in C_{a_i(t-1)}$. \square

4. Cooperative search and surveillance with multiple UAVs

To construct the map of an entirely unknown area, UAVs usually perform measurements through coordinated motion. On the one hand, UAVs perform motion control cooperatively to maximize the event occurrence detection probability. On the other hand, UAVs gather information from detected data sources and conduct information fusion through interactions with its neighboring UAVs. In this section, an alternative way to consistently estimate the target distribution using the Bayes rules is introduced. Then a consensus-based algorithm is introduced to construct the vehicles' probability map by incorporating both current observations of their neighbors and their historical estimations. Besides, the probability map is associated with the uncertainty, which guides the following coordinated motion.

4.1. Probability map updating based on sensor observations

We first describe the probability updating process using the Bayes rule without information sharing. Each vehicle v_i keeps an individual probability map of all the cells in the region of interest $P_{i,g,t} = P_{i,t}$ ($\theta_g = 1$), where $\theta_g = 1$ denotes the event that a target is present in cell g and $\theta_g = 0$ indicates that no target is present in that cell. A vehicle constructs its individual map $P_{i,g,t}$ according to sensor readings up to time t .

According to the Bayes formula, the probability that a target is present in cell g , $P(\theta_g = 1 | Z_{i,g,t})$, takes the form that

$$P(\theta_g = 1 | Z_{i,g,t}) = \frac{P(Z_{i,g,t} | \theta_g = 1)P(\theta_g = 1)}{P(Z_{i,g,t})} \quad (21)$$

where $P(\theta_g = 1)$ is the required prior probability of the target state in cell g . It is reasonable to take history estimations of the probability at the previous time, $P_{i,g,t-1}$, as the prior probability. Combining sensor observation $Z_{i,g,t}$ and prior probability $P_{i,g,t-1}$, we can estimate the probability $P_{i,g,t}$ as follows

$$P_{i,g,t} = \frac{P(Z_{i,g,t} | \theta_g = 1)P_{i,g,t-1}}{P(Z_{i,g,t})}. \quad (22)$$

Note that we set the initial value of P_{i,g,t_0} as 0.5 since v_i knows nothing about the mission area before starting the search. The denominator in Eq. (22) can be calculated using the law of total probability

$$P(Z_{i,g,t}) = P(Z_{i,g,t} | \theta_g = 1)P(\theta_g = 1) + P(Z_{i,g,t} | \theta_g = 0)P(\theta_g = 0) \quad (23)$$

where $P(Z_{i,g,t} | \theta_g = 1)$ and $P(Z_{i,g,t} | \theta_g = 0)$ quantitatively describe the probability of occurrence for an observation result under certain target present situations. Here we adopt two parameters to characterize the sensor's performance: detection probability $p_c = P(Z_{i,g,t} = 1 | \theta_g = 1)$ and false alarm probability $p_f = P(Z_{i,g,t} = 1 | \theta_g = 0)$, respectively.

By substituting Eq. (22) into Eq. (23), we can get the map construction rule, which associates the sensor observation $Z_{i,g,t}$ with estimation of the individual probability map $P_{i,g,t}$, which is written as

$$\begin{aligned} P_{i,g,t} &= P(\theta_g = 1 | Z_{i,g,t}) \\ &= \frac{P(Z_{i,g,t} | \theta_g = 1)P(\theta_g = 1)}{P(Z_{i,g,t} | \theta_g = 1)P(\theta_g = 1) + P(Z_{i,g,t} | \theta_g = 0)P(\theta_g = 0)} \\ &= \begin{cases} \frac{p_c P_{i,g,t-1}}{p_c P_{i,g,t-1} + p_f(1 - P_{i,g,t-1})} & \text{if } Z_{i,g,t} = 1 \\ \frac{(1 - p_c)P_{i,g,t-1}}{(1 - p_c)P_{i,g,t-1} + (1 - p_f)(1 - P_{i,g,t-1})} & \text{if } Z_{i,g,t} = 0 \\ P_{i,g,t-1} & \text{otherwise.} \end{cases} \end{aligned} \quad (24)$$

In the following parts, we mainly consider the general case where $0 < p_c < 1$ and $0 < p_f < 1$. To reduce the computational complexity, we introduce the following nonlinear transformation of $P_{i,g,t}$, which takes the form

$$H_{i,g,t} = \ln\left(\frac{1}{P_{i,g,t}} - 1\right). \quad (25)$$

Consequently, Eq. (24) can be transformed into

$$H_{i,g,t} = \begin{cases} H_{i,g,t-1} + \ln \frac{p_f}{p_c} & \text{if } Z_{i,g,t} = 1 \\ H_{i,g,t-1} + \ln \frac{1-p_f}{1-p_c} & \text{if } Z_{i,g,t} = 0 \\ H_{i,g,t-1} & \text{otherwise.} \end{cases} \quad (26)$$

In this condition, the update rule in Eq. (24) is transformed into a linear function of $H_{i,g,t}$, which only involves simple summations and has significantly reduced the computational complexity. We should also note that Eq. (25) is a bijective transformation of $P_{i,g,t} \in (0, 1)$. This formulation has established a one-to-one correspondence between the target distribution probability $P_{i,g,t}$ and the stored information $H_{i,g,t}$, allowing us to recover $P_{i,g,t}$ from $H_{i,g,t}$ uniquely whenever needed.

4.2. Consensus-based filter for cooperative information fusion

To further enhance the search efficiency, vehicles can update their probability maps cooperatively through information exchange [36]. We perform the fusion of sensor observations by introducing a simple consensus-like distributed scheme, which guarantees probability maps of all the vehicles converge to the same one that reflects the actual existence or nonexistence of targets under connected conditions or independent link failure conditions.

As we have described in the previous section, the individual map $H_{i,g,t}$ could be updated by incorporating new sensor readings using the Bayes rule. Subsequently, each vehicle transmits its updated probability map to its neighbors, which contains both new observation and historical target information. Then, UAVs fuse the probability map with a linear combination of its knowledge and the received information by the following rule:

$$Q_{i,g,t} = \omega_{i,i,t} H_{i,g,t} + \sum_{j \in N_{i,t}} \omega_{i,j,t} H_{j,g,t} \quad (27)$$

where $\omega_{i,j,t}$ is the weight on $H_{j,g,t}$ and N_i is the neighbor set of v_i . The above equation can be reformulated into compact form by setting $\omega_{i,j,t} = 0$ for all $v_j \notin N_i$, which can be written as

$$Q_{i,g,t} = \sum_{j=1}^n \omega_{i,j,t} H_{j,g,t}. \quad (28)$$

Here $W_t = (\omega_{i,j,t})$ is the well-known Metropolis weight matrix [37,38], given by

Table 1

Procedures of multiple UAV cooperative search using the proposed potential game approach.

```

1   Name: Cooperative search using multiple UAVs
2   Goal: Maximize area coverage and data collection
3   Requires: Limited sensing and communication capabilities
4
5   1 The mission region is uniformly portioned into  $M$  cells and each vehicle is initialized with an individual map  $Q$ 
6   2 While the mission space  $\mathcal{Q}$  is not fully understood do
7   3   /*Optimal coverage using binary log-linear learning*/
8   4   For all UAVs in the player set  $V$  do
9   5       Randomly select a vehicle  $v_i \in V$  from the player set
10  6       Choose a trial action  $a'_i(t)$  from the constrained action set,  $a'_i(t) \in C_{a_i(t-1)}$ 
11  7       The selected vehicle  $v_i$  computes its current utility  $U_i(a(t-1))$  and the expected utility  $U_i(a'_i, a_{-i}(t-1))$  according to Eq. (5)
12  8       Vehicle  $v_i$  choose an action according to the calculated utilities Eq. (8)
13  9       Vehicle  $v_i$  decides which direction to move toward based on  $a_i(t)$ 
14 10   End For
15 11   /*Sensor observations and information fusion*/
16 12   For each vehicle in the player set  $v_i \in V$  do
17 13       Performs observations  $Z_{i,g,t}$  over regions within its sensing range
18 14       Updates its individual map  $H_{i,g,t}$  using observed sensor readings according to Eq. (26)
19 15       Transmits its updated map  $H_{i,g,t}$  to its neighbors determined by its communication range
20 16       Performs information fusion based on Eq. (28)
21 17       Update the uncertainty map  $\eta_{i,g,t}$  according to the fused information to direct the motion control
22 18   End For
23 19    $t = t + 1$ 
24 20   End While

```

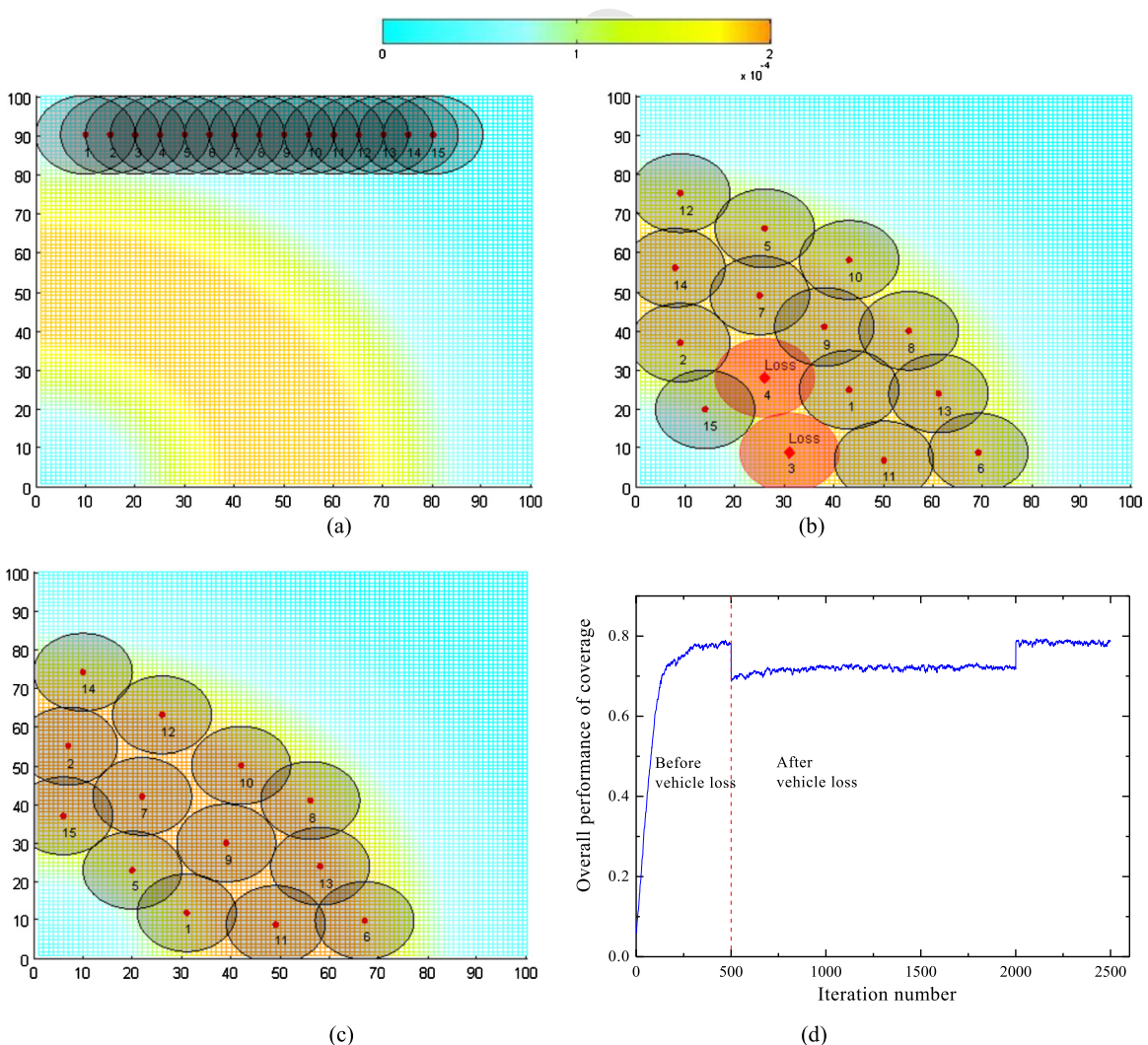


Fig. 4. Optimal coverage with 15 homogeneous UAVs. (a) Locations of vehicles before the operation. (b) The configuration after 500 learning steps, highlighted red circles are failed vehicles. (c) The final reconfiguration in the case of vehicle losses. (e) Evolution curve of the potential function. (For interpretation of the references to color in this figure legend, the reader is referred to the web version of this article.)

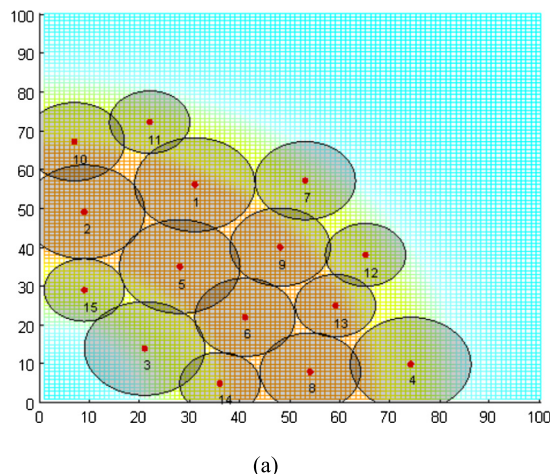


Fig. 5. Optimal coverage with 15 heterogeneous UAVs. (a) The final configuration of the coverage. (b) Evolution curve of the potential function.

$$\omega_{i,j,t} = \begin{cases} \frac{1}{1+\max\{\kappa_i, \kappa_j\}} & \text{if } \{v_i, v_j\} \in E \\ 1 - \sum_{\{v_i, v_k\} \in E} \omega_{i,k,t}(t) & \text{if } i = j \\ 0 & \text{otherwise} \end{cases} \quad (29)$$

where κ_i and κ_j are degrees of vehicle v_i and v_j , respectively. And E is the edge set of the resulting network. It is worth mentioning that the weight matrix $W_t \in R^{n \times n}$ has sparsity pattern, which can be utilized to reduce the storage requirement. If the resulting network is connected, then W_t is an ergodic doubly stochastic matrix [38], which guarantees asymptotic convergence to the average consensus.

Here we will cite a theorem concerning the convergence property of the distributed consensus-based fusion process using the Metropolis weight matrix [37].

For the distributed information fusion process defined by Eq. (28), an average consensus is asymptotically reached for all initial state Q_{i,g,t_0} , with the limit

$$\lim_{t \rightarrow \infty} Q_{i,g,t} = \frac{1}{n} \sum_{i=1}^n Q_{i,g,t_0}, \quad \forall v_i \in V.$$

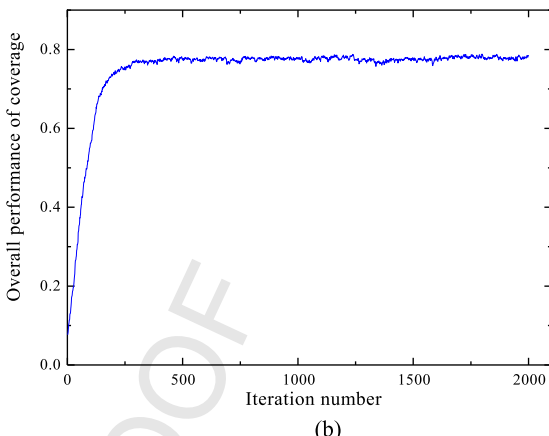
If UAVs performing the cooperative search satisfy one of the following two properties:

- (i) The communication topology of UAVs constitutes a connected network.
- (ii) The communication topology of UAVs constitutes a connected network with independent link failures.

4.3. A potential game approach to cooperative search and surveillance

For the surveillance problem, UAVs aim at maximizing the event occurrence detection probability with the help of onboard sensors. The problem of monitoring an area of interest is substantially identical to covering the same area. However, searching an unknown area is more difficult since it involves data source detection and data collection in addition to sensor deployment. In this work, we try to address both the problem of cooperative surveillance and search using multiple UAVs.

Initially, each vehicle keeps an individual probability map $P_{i,g,t}$ of the mission area, which describes the probability of the existence of a target for a particular cell g . Since the problem has been formulated as a potential game, each vehicle performs coordinated motion by adhering to the binary log-linear learning rule. After vehicle v_i is deployed to a new location, it performs observation $Z_{i,g,t}$ to collect data and updates its individual probability map



$P_{i,g,t}$ accordingly. To further enhance the search effectiveness, v_i refreshes its knowledge $Q_{i,g,t}$ through information exchange with its neighbors. We have noticed that its knowledge $\|Q_{i,g,t}\|$ provides a good measure of uncertainty. More precisely, it is straightforward to check that the larger $\|Q_{i,g,t}\|$, the less uncertainty v_i has about information of target existence, and vice versa. Similar to [22], we define the density function in Eq. (3) as,

$$\eta_{i,g,t} = e^{-k_\eta \|Q_{i,g,t}\|}, \quad (30)$$

where k_η represents the positive gain and $\eta_{i,g,t}$ denotes the uncertainty map.

With $Q_{i,g,t}$ included into density map η , UAVs tend to move to locations with high uncertainty, which in turn reduces the uncertainty by incorporating new sensor observations. Then UAVs repeat coordinated motion and cooperative information fusion until uncertainty distributions over all the cells in the mission space fall below a predetermined threshold. The detailed procedures to implement cooperative search using multiple UAVs are illustrated in Table 1.

5. Simulation results and discussions

Simulations are carried out to validate the effectiveness of the potential game based approach to cooperative search and surveillance with multiple UAVs. We first focus on the scenario where UAVs aim at covering a mission area with prior knowledge for surveillance purposes. For this purpose, we demonstrate the optimal coverage problem using both homogeneous and heterogeneous UAVs. Then we further investigate the scenario for coverage over mission areas with four obstacles. We also verify the performance of cooperative search using our proposed approach. To gain more insight into how parameters affects the search effectiveness, we elaborated on this subject further by examining the convergence properties of the search process. All experiments are carried out on a personal computer with Intel Core Duo CPU T6600, 4 GB memory and Windows 7 under MATLAB (Release R2010a).

5.1. Cooperative surveillance for an area with prior knowledge

Consider an optimal coverage problem, aiming at deploying n UAVs to maximize expected event detection probability. The mission area Ω is divided into 100×100 cells uniformly, and the probability an event occurs in each cell is specified by a predetermined density function η over Ω . We assume that $\eta(g) \geq 0$, $\forall g \in \Omega$, where $\sum_{g \in \Omega} \eta(g) = 1$. Color-coded representation of the density map for the mission area is illustrated in Fig. 4. Here we

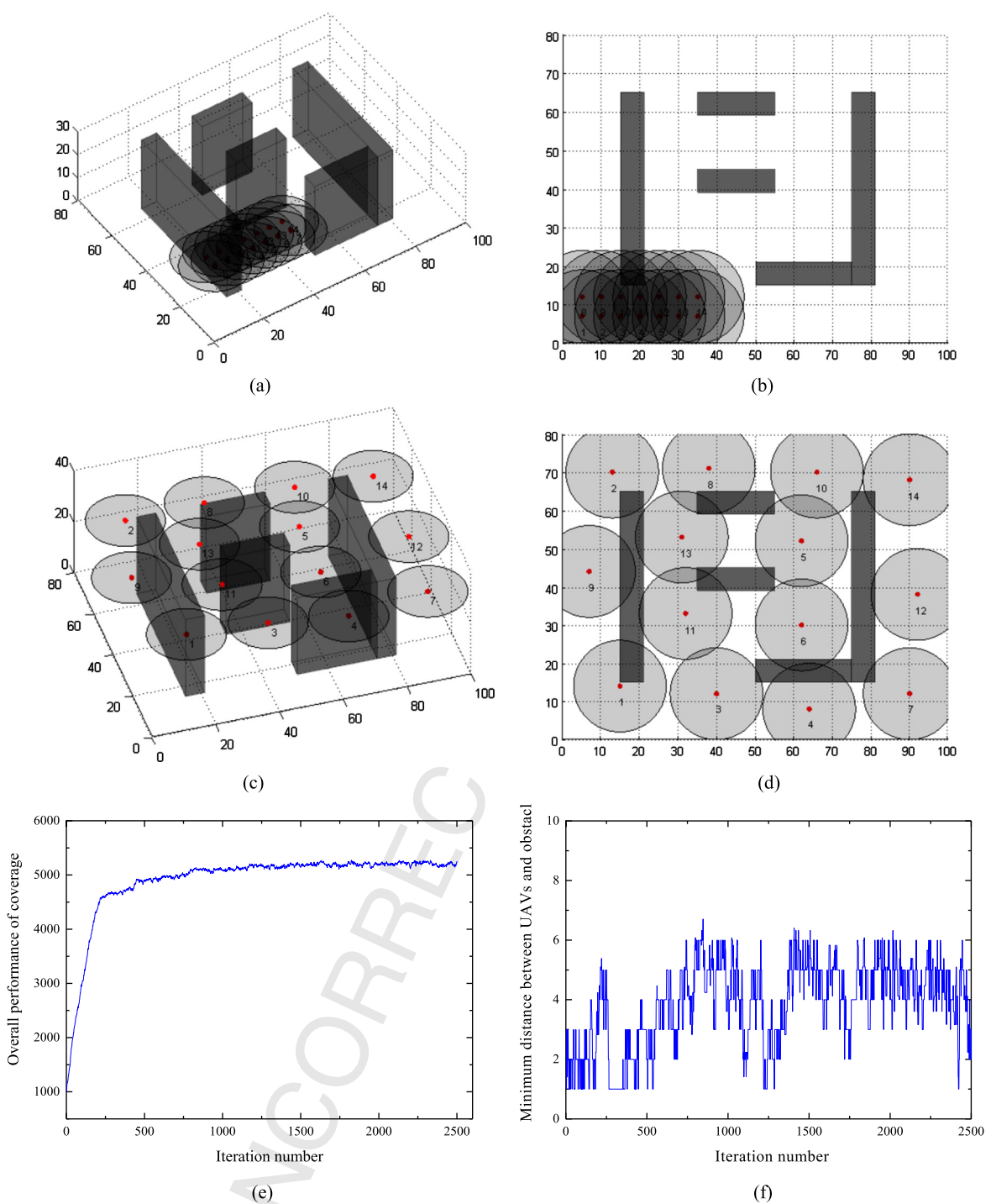
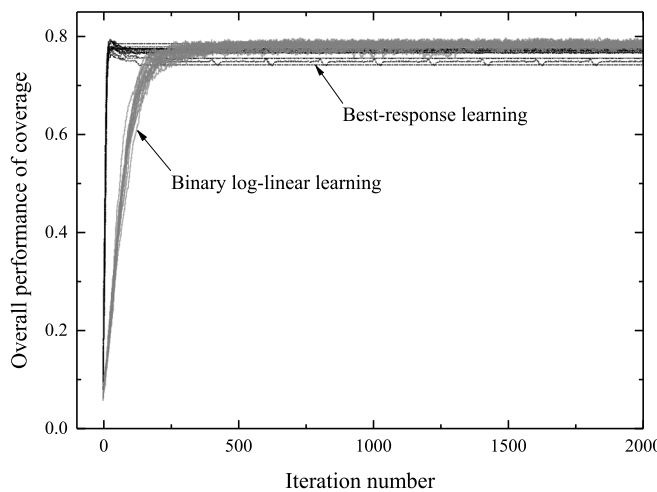


Fig. 6. Optimal coverage over a mission area with four obstacles. (a) Initial locations of the vehicles (side view). (b) Initial locations of the vehicles (top view). (c) Final configuration after the cooperative search (side view). (d) Final configuration after the cooperative search (top view). (e) Evolution curve of the potential function. (f) Minimum distance between all the UAVs and obstacles.

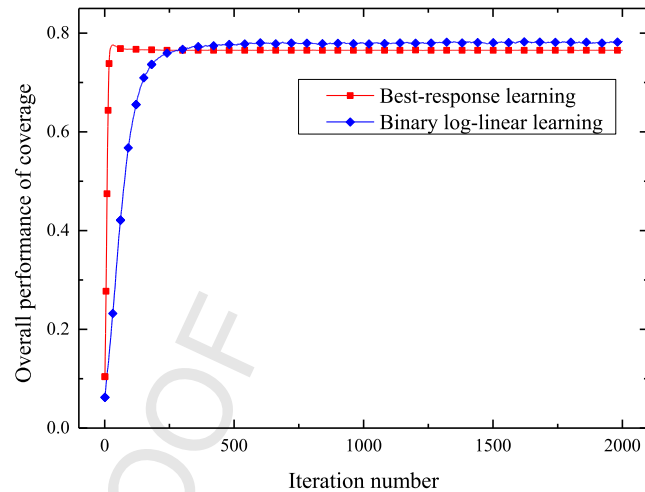
use 15 UAVs to cover the mission space autonomously, whereby each vehicle has a sensing radius of 10-m. Initially, each vehicle is uniformly distributed at one side of the mission area, as is shown in Fig. 4(a). Note that different started locations have no effects on the final configuration and do not change our main conclusions. Each vehicle is endowed with an individual utility function defined by Eq. (4) and adheres to binary log-linear learning to change their locations. Each vehicle seeks to maximize the margin contribution according to Eq. (8), where the temperature $\tau = 0.2$. The final configuration of UAVs is shown in Fig. 4(b).

To evaluate the robustness of our proposed algorithm, we further investigate the situations of unexpected failures. Highlighted red circles in Fig. 4(b) represent the two failed UAVs. The remaining UAVs begin to adjust their locations autonomously when they have detected the vehicle losses. As we can see from Fig. 4(c) and Fig. 4(d), UAVs reconfigure themselves to the optimal coverage successfully through binary log-linear learning.

Here we have also examined the performance of coverage with 15 heterogeneous UAVs, where 5 UAVs have the sensing range of 12 m, 5 UAVs have the sensing range of 10-m, and the left 5 UAVs

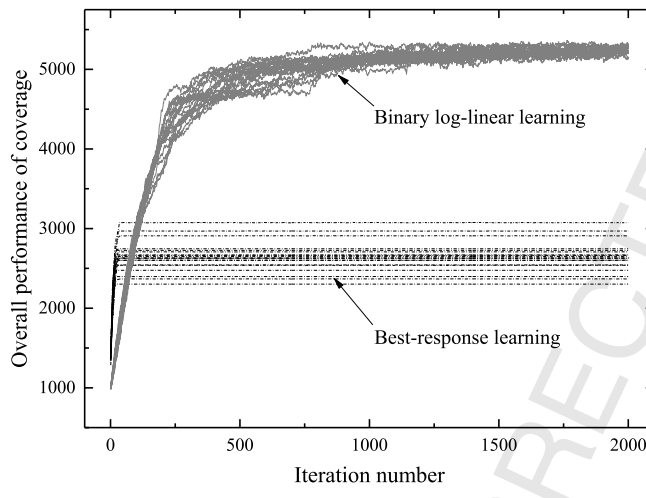


(a)

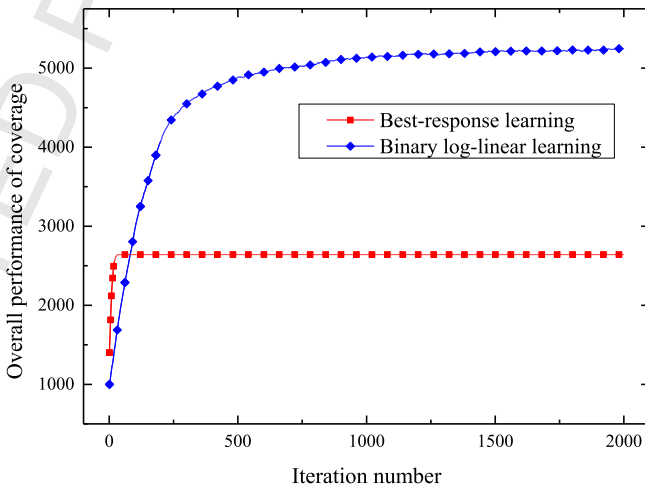


(b)

Fig. 7. Comparative results for best-response learning and binary log-linear learning for the case in Fig. 4. (a) Evolutionary curves of the potential function in each run. (b) Averaged evolutionary curves of the potential function.



(a)



(b)

Fig. 8. Comparative results for best-response learning and binary log-linear learning for the case in Fig. 6. (a) Evolutionary curves of the potential function in each run. (b) Averaged evolution curves of the potential function.

have the sensing range of 8 m. The final configuration to monitor an area of interest is illustrated in Fig. 5(a). To provide a quantitative measurement of the overall performance, we demonstrate evolution processes of the potential function in Fig. 5(b). Note that the potential function is optimized continually during the learning process despite the presence of some fluctuations, which is consistent with the snapshots in Fig. 4(d).

To evaluate the effectiveness of the proposed approach in unknown environments with obstacles, we define a mission area with four obstacles. The shaded polygons represent the obstacles, as depicted in Fig. 6(a). Again, the mission space is portioned into 100×80 cells uniformly, and UAVs move according to the action constructed by their current positions. Here we will focus on covering this area as large as possible for monitoring or surveillance purposes, which is somewhat similar to the case in Fig. 4 and Fig. 5. The final configuration of UAVs is depicted by Fig. 6(c) (side view) and Fig. 6(d) (top view). The minimum relative distances between the obstacles (including boundaries of the mission area) and the UAVs are shown Fig. 6(f).

To inspect the effectiveness of our approach, we compare the binary log-linear learning with the well-known best-response

learning in game theory. The simulations are carried out for covering an area of interest with or without obstacles (scenarios in Fig. 4 and Fig. 6). To eliminate effects of stochastic ingredients in learning processes, we run each algorithm for 20 times, as is shown in Figs. 7–8. As expected, vehicles utilizing the best-response rules outperform the binary log-linear learning at the beginning. However, it can be easily observed that the binary log-linear learning demonstrates better coverage performance in both cases, especially in the environment with obstacles. Under the best-response dynamics, vehicles tend to act according to their individual interests and are easy to be trapped into local optima. We should note that fluctuations of learning curves for binary log-linear learning are crucial for optimizing the collective behavior. The fluctuation is introduced by τ , which allows vehicles to make mistakes occasionally and endow them with capabilities to escape from local optima. Note that τ can set to be time-varying to characterize the tradeoff between the exploration of new solutions and the exploitation of already discovered solutions. In this way, UAVs achieve a state that maximizes the potential function, which we can see in Theorem 1. Importantly, the binary log-linear learning is more computational efficient because the best-response

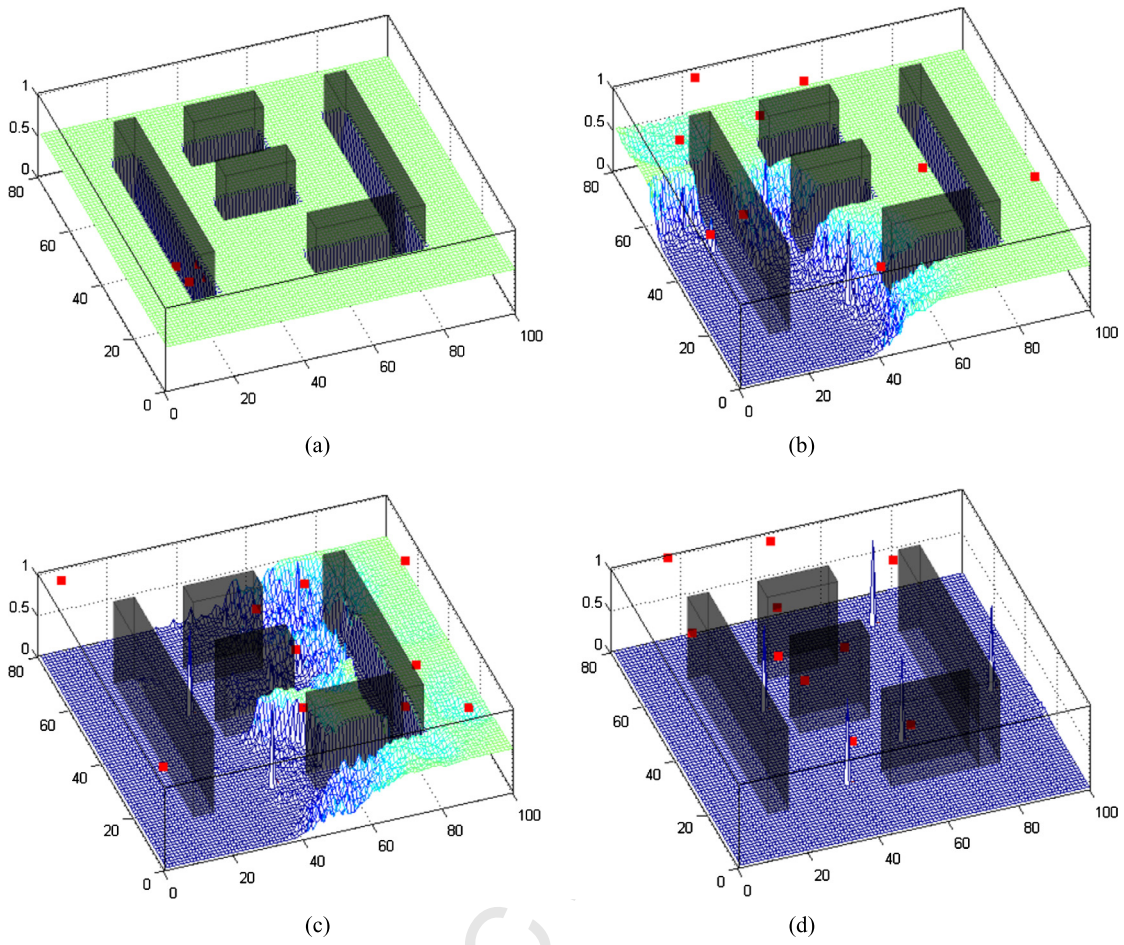


Fig. 9. Snapshots of the probability map for one vehicle. (a) Time step $t = 0$. (b) Time step $t = 200$. (c) Time step $t = 500$. (d) Time step $t = 1500$.

learning requires calculating expected utilities of all the candidate actions.

5.2. Cooperative search for an unknown area

First, we will provide the readers with some intuition by demonstrating the vehicle's probability map constructed by cooperative search. For the sake of simplicity, we illustrate the snapshots of one vehicle since the remaining UAVs have qualitatively similar results, as is shown in Fig. 9. Initially, the probability that a target is present in any cell g for vehicle v_i is $P_{i,g,t_0} = 0.5$, indicating that it has no prior information about the mission space. As the search goes on, probabilities in cells without targets converge to 0, and those in cells with targets converge to 1.

Since UAVs gain information about the mission space by reducing the uncertainty of each cell, the convergence of the individual probability map $P_{i,g,t}$ of vehicle v_i implies that uncertainty $\eta_{i,g,t}$ approaches 0. Consequently, the average uncertainty form $\bar{\eta}_t = (1/nM) \sum_{i=1}^n \sum_{g \in \Omega} \eta_{i,g,t}$ serves as an appropriate measure of the search performance. It is easy to check that the initial value of $\bar{\eta}_t$ is $\bar{\eta}_0 = 1$.

In what follows, we examined the time evolution cause of average uncertainty for different parameters to distinguish possible factors that may affect the search performance. Simulations for cooperative search are carried out to investigate the effect of the number of UAVs, onboard sensor performance, and the sampling frequency. We assume that UAVs perform sensor observations synchronously and communicate with their neighbors immediately after they have updated the probability map. So here we adopt the notation sampling frequency F_S to represent that UAVs take

Table 2
Parameter settings for comparison simulations.

	Case 1	Case 2	Case 3	Case 4
Number of UAVs n	8, 10, 12	10	10	10
Sensing radius R_S , m	10	8, 9, 10	10	10
Communication radius R_C , m	40	40	40	40
Detection probability p_c	0.9	0.9	0.7, 0.8, 0.9	0.9
False alarm probability p_f	0.3	0.3	0.3	0.3
Sensing frequency F_S	1	1	1	2, 4, 6

an observation after how many steps they move. In the first case, we use different numbers of UAVs to perform the search to inspect the effect of scalability on the search performance. Next, we analyze effects of onboard sensor properties and sampling frequency in three other cases, and relevant simulation parameters are shown in detail in Table 2. In addition to the parameters mentioned above, we set the probability map $Q_{i,g,t_0} = 0$ for all UAVs and cells g , gain the parameter $k_\eta = 1$, the temperature in binary log-linear learning $\tau = 0.2$, and the predefined threshold for termination $\delta_0 = 10^{-5}$. The final results below are averaged over 20 realizations for each set of parameters.

Fig. 10 shows experimental results of the average uncertainty of the entire vehicle network for different parameter settings. As can be seen in Fig. 10(a), the convergence speed increases slightly as the number of UAVs increases, which is somewhat reasonable since operations with multiple vehicles provide comprehensive information when taking a measurement. Especially, it is easy for the proposed approach to scale to large numbers of UAVs without increasing the design complexity. In analogy to the previous case, we can observe a qualitatively similar result, that is, the search op-

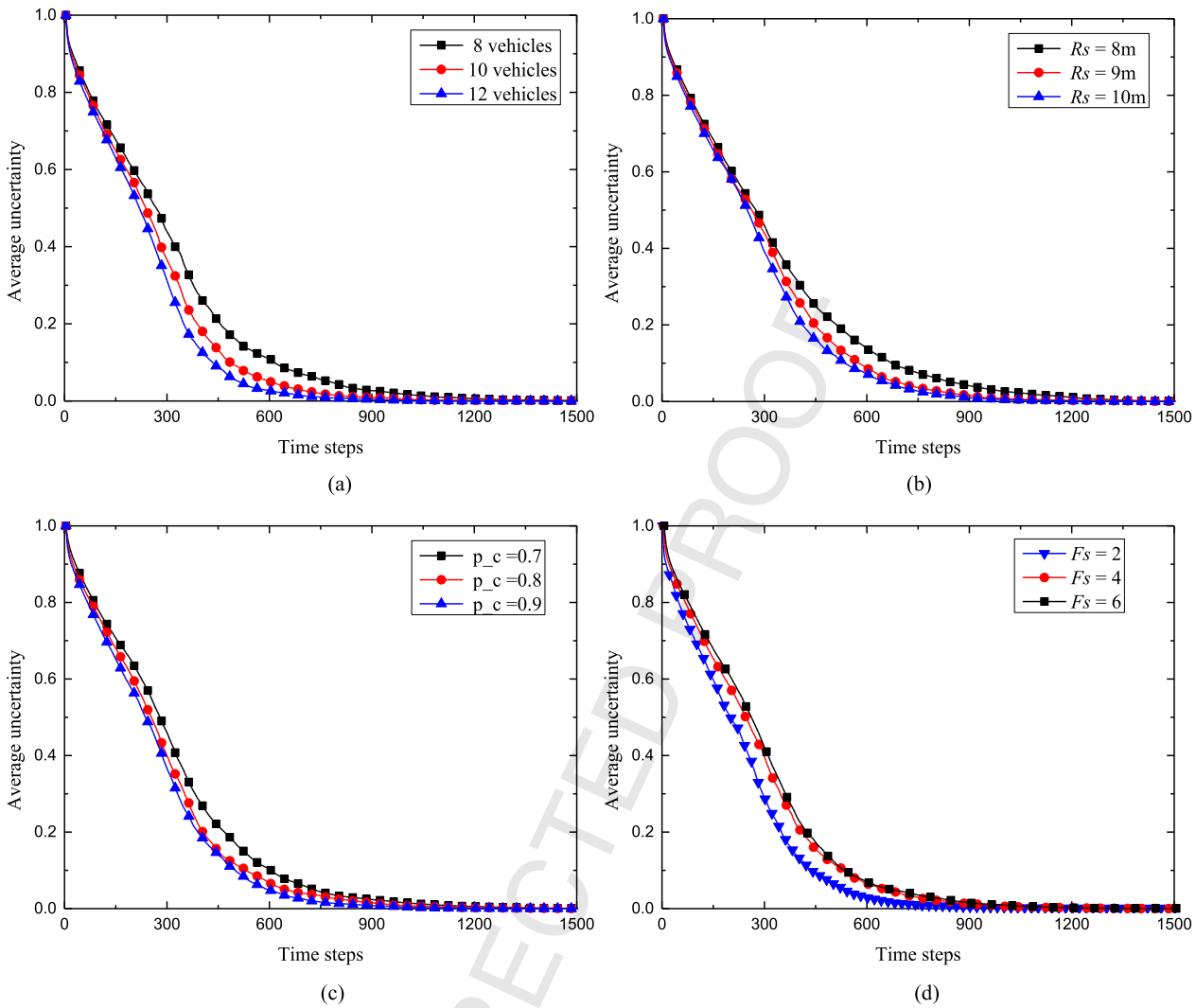


Fig. 10. Time evolution course of average uncertainty for different parameters. (a) Different vehicle numbers n . (b) Different sensing radius R_s . (c) Different correct detection probability p_c . (d) Different sampling frequency F_s .

eration could be performed more efficiently by applying sensors with stronger sensing capabilities, such as larger sensing radius (Fig. 10(b)), or higher correct detection probabilities (Fig. 10(c)). Furthermore, increasing the sample frequency promotes the search efficiency, whereas it may result in more computational burden, higher bandwidth capacity, and more energy consumption. Hence, this parameter should be carefully tailored to balance the effectiveness and complexity tradeoff. It is also noteworthy that the average uncertainty converges to 0 (under predefined threshold δ_0) for most cases, suggesting that UAVs obtain good knowledge about the mission space.

6. Conclusions

We developed a potential game formulation for cooperative search and surveillance using multiple UAVs. By designing the coordinated motion as a multi-player potential game with constrained action sets, we view UAVs as decision makers that operate autonomously in a distributed fashion. The binary log-linear learning is adopted to perform motion control, which guarantees convergence to the optimal configuration. Moreover, a simple iterative distributed fusion algorithm based on a consensus filter is introduced to construct the probability map. The probability map is associated with the uncertainty of the mission area, which in turn guides the following coordinated motion. The modular framework

of our proposed approach enables the separate design of utility functions and learning algorithms, which offers a flexible way to accommodate different global objectives and physical constraints. This formulation also makes it suitable for implementation with heterogeneous UAVs and in mission areas with obstacles without including additional treatment. We will focus on the application of our proposed approach in actual flight tests considering kinematics and dynamics of UAVs in the following work.

Conflict of interest statement

The authors declare that there is no conflict of interests regarding the publication of this article.

Acknowledgements

This work was partially supported by National Natural Science Foundation of China (NSFC) (Grant Nos. 61425008, 61333004), Aeronautical Foundation of China (Grant No. 2015ZA51013), and the Academic Excellence Foundation of BUAA for PhD Students.

References

- [1] B. Jiang, A.N. Bishop, B.D. Anderson, S.P. Drake, Optimal path planning and sensor placement for mobile target detection, *Automatica* 60 (2015) 127–139.

- [2] K. Guruprasad, D. Ghose, Deploy and search strategy for multi-agent systems using Voronoi partitions, in: Proceedings of 4th International Symposium on Voronoi Diagrams in Science and Engineering, IEEE, Glamorgan, 2007, pp. 91–100.
- [3] M. Jadalha, J. Choi, Environmental monitoring using autonomous aquatic robots: sampling algorithms and experiments, *IEEE Trans. Control Syst. Technol.* 21 (2013) 899–905.
- [4] H.M. La, W. Sheng, J. Chen, Cooperative and active sensing in mobile sensor networks for scalar field mapping, *IEEE Trans. Syst. Man Cybern.* 45 (2015) 1–12.
- [5] A.C. Kapoutsis, S.A. Chatzichristofis, L. Doitsidis, J.B. de Sousa, J. Pinto, J. Braga, E.B. Kosmatopoulos, Real-time adaptive multi-robot exploration with application to underwater map construction, *Auton. Robots* 40 (2016) 987–1015.
- [6] H.M. La, W. Sheng, Distributed sensor fusion for scalar field mapping using mobile sensor networks, *IEEE Trans. Cybern.* 43 (2013) 766–778.
- [7] M.M. Polycarpou, Y. Yang, K.M. Passino, A cooperative search framework for distributed agents, in: Proceedings of the 2001 IEEE International Symposium on Intelligent Control, IEEE, Mexico City, 2001, pp. 1–6.
- [8] H. Duan, S. Liu, Non-linear dual-mode receding horizon control for multiple unmanned air vehicles formation flight based on chaotic particle swarm optimisation, *IET Control Theory Appl.* 4 (2010) 2565–2578.
- [9] B. Di, R. Zhou, H. Duan, Potential field based receding horizon motion planning for centrality-aware multiple UAV cooperative surveillance, *Aerosp. Sci. Technol.* 46 (2015) 386–397.
- [10] S. Martinez, J. Cortes, F. Bullo, Motion coordination with distributed information, *IEEE Control Syst.* 27 (2007) 75–88.
- [11] S. Kar, J.M. Moura, Distributed consensus algorithms in sensor networks with imperfect communication: link failures and channel noise, *IEEE Trans. Signal Process.* 57 (2009) 355–369.
- [12] M. Zhong, C.G. Cassandras, Distributed coverage control and data collection with mobile sensor networks, *IEEE Trans. Autom. Control* 56 (2011) 2445–2455.
- [13] L. Ambroziak, Z. Gosiewski, Two stage switching control for autonomous formation flight of unmanned aerial vehicles, *Aerosp. Sci. Technol.* 46 (2015) 221–226.
- [14] J. Cortés, S. Martinez, T. Karatas, F. Bullo, Coverage control for mobile sensing networks, *IEEE Trans. Robot. Autom.* 20 (2004) 243–255.
- [15] F. Bullo, J. Cortes, S. Martinez, *Distributed Control of Robotic Networks: A Mathematical Approach to Motion Coordination Algorithms*, Princeton University Press, Princeton, NJ, 2009.
- [16] H. Duan, P. Li, *Bio-inspired Computation in Unmanned Aerial Vehicles*, Springer-Verlag, Berlin, Heidelberg, 2014.
- [17] R.W. Beard, T.W. McLain, Multiple UAV cooperative search under collision avoidance and limited range communication constraints, in: Proceedings of 42nd IEEE Conference on Decision and Control, IEEE, Hawaii, 2003, pp. 25–30.
- [18] R. Olfati-Saber, R.M. Murray, Consensus problems in networks of agents with switching topology and time-delays, *IEEE Trans. Autom. Control* 49 (2004) 1520–1533.
- [19] J. Cortes, S. Martinez, F. Bullo, Spatially-distributed coverage optimization and control with limited-range interactions, *ESAIM Control Optim. Calc. Var.* 11 (2005) 691–719.
- [20] W. Burgard, M. Moors, C. Stachniss, F.E. Schneider, Coordinated multi-robot exploration, *IEEE Trans. Robot.* 21 (2005) 376–386.
- [21] F. Zhang, N.E. Leonard, Cooperative filters and control for cooperative exploration, *IEEE Trans. Autom. Control* 55 (2010) 650–663.
- [22] J. Hu, L. Xie, K.-Y. Lum, J. Xu, Multiagent information fusion and cooperative control in target search, *IEEE Trans. Control Syst. Technol.* 21 (2013) 1223–1235.
- [23] P. Sujit, D. Ghose, Self assessment-based decision making for multiagent cooperative search, *IEEE Trans. Autom. Sci. Eng.* 8 (2011) 705–719.
- [24] J.R. Marden, G. Arslan, J.S. Shamma, Cooperative control and potential games, *IEEE Trans. Syst. Man Cybern., Part B, Cybern.* 39 (2009) 1393–1407.
- [25] L.M. De Campos, J.M. Fernandez-Luna, J.A. Gámez, J.M. Puerta, Ant colony optimization for learning Bayesian networks, *Int. J. Approx. Reason.* 31 (2002) 291–311.
- [26] J.R. Marden, J.S. Shamma, Revisiting log-linear learning: asynchrony, completeness and payoff-based implementation, *Games Econ. Behav.* 75 (2012) 788–808.
- [27] N. Li, J.R. Marden, Designing games for distributed optimization, *IEEE J. Sel. Top. Signal Process.* 7 (2013) 230–242.
- [28] D. Monderer, L.S. Shapley, Potential games, *Games Econ. Behav.* 14 (1996) 124–143.
- [29] J.F. Nash, Equilibrium points in n -person games, *Proc. Natl. Acad. Sci. USA* 36 (1950) 48–49.
- [30] J.R. Marden, State based potential games, *Automatica* 48 (2012) 3075–3088.
- [31] G. Arslan, J.R. Marden, J.S. Shamma, Autonomous vehicle-target assignment: a game-theoretical formulation, *J. Dyn. Syst. Meas. Control* 129 (2007) 584–596.
- [32] J.R. Marden, G. Arslan, J.S. Shamma, Joint strategy fictitious play with inertia for potential games, *IEEE Trans. Autom. Control* 54 (2009) 208–220.
- [33] D. Fudenberg, D.K. Levine, *The Theory of Learning in Games*, MIT Press, Cambridge, MA, 1998.
- [34] J.R. Marden, G. Arslan, J.S. Shamma, Connections between cooperative control and potential games illustrated on the consensus problem, in: Proceedings of European Control Conference, Kos, Greece, 2007, pp. 4604–4611.
- [35] S. Boyd, A. Ghosh, B. Prabhakar, D. Shah, Randomized gossip algorithms, *IEEE Trans. Inf. Theory* 52 (2006) 2508–2530.
- [36] P. Yang, R.A. Freeman, K.M. Lynch, Distributed cooperative active sensing using consensus filters, in: Proceedings of IEEE International Conference on Robotics and Automation, IEEE, Rome, Italy, 2007, pp. 405–410.
- [37] L. Xiao, S. Boyd, S. Lall, A scheme for robust distributed sensor fusion based on average consensus, in: Proceedings of 4th International Symposium on Information Processing in Sensor Networks, IEEE, Los Angeles, California, USA, 2005, pp. 63–70.
- [38] Z. Li, F.R. Yu, M. Huang, A distributed consensus-based cooperative spectrum-sensing scheme in cognitive radios, *IEEE Trans. Veh. Technol.* 59 (2010) 383–393.

67
68
69
70
71
72
73
74
75
76
77
78
79
80
81
82
83
84
85
86
87
88
89
90
91
92
93
94
95
96
97
98
99
100
101
102
103
104
105
106
107
108
109
110
111
112
113
114
115
116
117
118
119
120
121
122
123
124
125
126
127
128
129
130
131
132